

Constructing a stacked benthic $\delta^{18}\text{O}$ record

Daniel B. Karner, Jonathan Levine, Brian P. Medeiros,¹ and Richard A. Muller

Department of Physics, University of California, Berkeley, California, USA

Received 18 June 2001; revised 4 March 2002; accepted 4 March 2002; published XX Month 2002.

[1] Composite stacks were constructed by superimposing 6 to 13 benthic foraminiferal $\delta^{18}\text{O}$ records covering the period 0–850 ka. An initial timescale for each core was established using radioisotopic age control points and assuming constant sedimentation rates between these points. The average of these records is our 13-core “untuned” stack. Next, we matched the 41 kyr component of each record individually to variations in Earth’s obliquity. Four of the 13 records produced timescales that were inconsistent with one or more of the known radioisotopic ages. The nine remaining cores were averaged to create a “minimally tuned” stack. Six of the minimally tuned cores were assembled into a “tropical” stack. For each stack we estimated the uncertainty envelope from the standard deviation of the constituents. Spectral analysis of the three stacks indicates that benthic $\delta^{18}\text{O}$ is dominated by a 100 kyr oscillation that has a narrow spectral peak. The contribution of precession to the total variance is small when compared to prior results from planktic stacks. *INDEX TERMS:* 3344 Meteorology and Atmospheric Dynamics: Paleoclimatology; 4804 Oceanography: Biological and Chemical: Benthic processes/benthos; 5416 Planetology: Solid Surface Planets: Glaciation; *KEYWORDS:* $\delta^{18}\text{O}$ stack, benthic foraminifera, obliquity tuning, spectral analysis, 100 kyr cycle, sea level

1. Introduction

[2] Sediment core records of $\delta^{18}\text{O}$ from foraminifera are some of the best data we have to study climate cycles. Since each record shows variations from local as well as global climate, a procedure was introduced in the 1970s called stacking. In this process, data from multiple cores are added to each other, with the expectation that global signals add coherently and local signals average out. Important $\delta^{18}\text{O}$ stacks include the pacemaker stack of *Hays et al.* [1976], the SPECMAP stack of *Imbrie et al.* [1984], the graphic correlation stack of *Prell et al.* [1986], and the low latitude stack of *Bassinot et al.* [1994]. Timescales are frequently deduced for new cores by correlation of their features to features in one of these stacks. These stacks have provided many insights toward understanding climate and have provided estimates of the timing and amplitude of climate cycles against which many theories have been compared.

[3] With the exception of the graphic correlation stack, which contains two benthic and 11 planktic $\delta^{18}\text{O}$ records, the stacks above are based exclusively on planktic $\delta^{18}\text{O}$ data from two (pacemaker), five (SPECMAP), and two (low latitude) sediment cores. In this paper, we stack $\delta^{18}\text{O}$ data from benthic foraminifera only. A priori, one might expect the benthic forams to be less susceptible to local climate conditions since localized variations are less likely to affect conditions in the deep ocean. The deep ocean, by virtue of its large volume and rapid mixing, dampens small-scale heterogeneity introduced from the surface. As there are only two principal sources of deep water, namely, North Atlantic Deep Water and Antarctic Bottom Water, large areas of the ocean floor are bathed with the same water masses. Additionally, the deep ocean is insulated from local sea surface temperature variations by the hundreds to thousands of meters of water above it.

[4] This insensitivity of benthic data to local climate has been argued by *Pisias et al.* [1984], *Chappell and Shackleton* [1986], and *Shackleton* [1987]. *Pisias et al.* [1984] constructed a 300 kyr

long stack of benthic $\delta^{18}\text{O}$ by forcing isotopic events in four cores into alignment with those in a reference core, V19-29. Unfortunately, two of the five cores in this stack only extend to ~ 150 ka. Data from a small region of the east equatorial Pacific are weighted heavily in this stack (three of the cores in this stack were from within 2° of each other), so it may have strong regional overprinting of the global signal. *Chappell and Shackleton* [1986] and *Shackleton* [1987] used averaged benthic $\delta^{18}\text{O}$ data, but their focus was not on construction of a global record; rather, they assessed $\delta^{18}\text{O}$ at specific times in order to estimate global sea level; they then compared their values with terrace elevation data.

[5] The prior stacks may not have successfully diminished local effects. The pacemaker stack [*Hays et al.*, 1976] used only two cores, and these were from the same region of the southern Indian Ocean; from this one does not expect much averaging out of local conditions. The SPECMAP stack [*Imbrie et al.*, 1984] was constructed using five planktic data sets from the Atlantic, Pacific, and Indian Oceans. However, two of these cores did not extend beyond 300 ka, and so beyond 300 ka the SPECMAP stack has limited suppression of local climate variations. The graphic correlation stack of *Prell et al.* [1986] used 13 $\delta^{18}\text{O}$ data sets, but 11 of these were of planktic foraminifera. Thus the benthic signal in the *Prell et al.* stack was suppressed by the overwhelming planktic signal. In the case of the low latitude stack, *Bassinot et al.* [1994] note that the planktic $\delta^{18}\text{O}$ in core MD900963 from the equatorial Indian Ocean records a global ice volume signal and a salinity signal related to the Indian monsoon. This core was averaged with only one other (Ocean Drilling Program (ODP) Site 677 from the east equatorial Pacific Ocean), and so the characteristic salinity variation of the Indian Ocean is unlikely to have been efficiently suppressed.

[6] The present paper takes advantage of the relatively recent acquisition of high-resolution $\delta^{18}\text{O}$ data that cover the past ~ 850 kyr. Each core included in this study was sampled by the original researchers every 2–6 kyr over the ~ 850 kyr period.

2. Climatic Significance of Benthic $\delta^{18}\text{O}$

[7] The use of planktic and benthic $\delta^{18}\text{O}$ as proxies for global ice volume has been a standard practice in paleoclimatology. Nonetheless, it has been acknowledged for some time that planktic

¹Now at Department of Atmospheric Sciences, University of California, Los Angeles, California, USA.

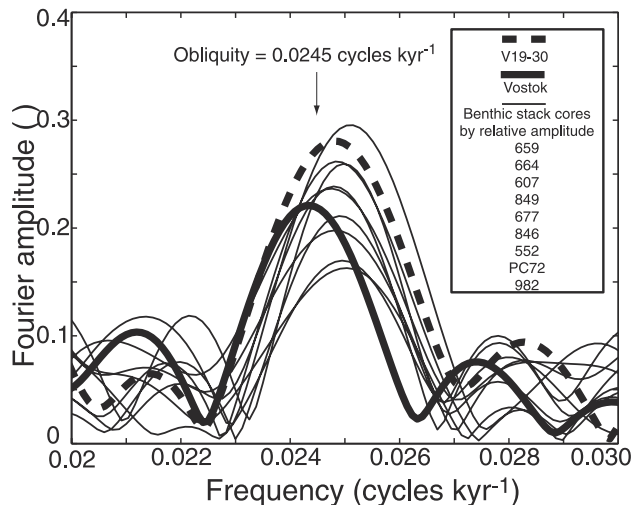


Figure 1. The spectral amplitude of obliquity in the time interval 0–420 ka for Vostok $\delta^{18}\text{O}_{\text{atm}}$ (tuned to 65°N summer insolation as suggested by *Petit et al.* [1999]) and benthic foraminiferal $\delta^{18}\text{O}$ data from cores V19-30 (using the timescale of *Imbrie et al.* [1992]) and nine of the cores analyzed here (based on our obliquity tuning described in the text and listed in order of decreasing spectral amplitude). *Shackleton* [2000] interprets the excess obliquity in core V19-30 relative to Vostok to represent the global paleotemperature signal in the deep ocean. However, the nine other deep-sea cores do not show a consistently larger 41 kyr oscillation in benthic $\delta^{18}\text{O}$ than in Vostok. These data show that it is not possible to accurately determine the global temperature contribution to the benthic $\delta^{18}\text{O}$ data from a single core.

data, and perhaps benthic data as well, contain significant salinity and temperature signals in addition to the ice volume signal [*Schrag et al.*, 1996; *Beck et al.*, 1997; *Hastings et al.*, 1998; *Elderfield and Ganssen*, 2000; *Lea et al.*, 2000; *Shackleton*, 2000]. Temperature change may affect both the planktic and benthic $\delta^{18}\text{O}$ values, accounting perhaps for up to 50% of the variability in benthic $\delta^{18}\text{O}$ [*Schrag et al.*, 1996; *Mashiotta et al.*, 1999; *Shackleton*, 2000], but these authors state that this estimate of the temperature effect remains uncertain because of the small number of records analyzed using their techniques. In our stacks we will show that the average change in benthic foraminiferal $\delta^{18}\text{O}$ since the Last Glacial Maximum is $\sim 1.3\%$. This agrees with the isotopic change of the oceans (1.26%) estimated by the accumulation of glaciers (volume

equivalent to 120 m of sea level change) with a $\delta^{18}\text{O}$ composition of -40% [*Broecker*, 1995]. However, *Schrag et al.* [1996] conclude that only 0.7–0.8‰ could be due to changes in the oxygen isotopic composition of the ocean water and thus to global ice volume, the remainder ($\sim 1\%$) being the result of a 4°C temperature change in the deep ocean. At present we do not believe the benthic stack created here will shed much light on the magnitude of this deep water temperature issue, and we do not choose to separate the temperature versus ice volume components of the benthic data. We will, however, compare the interglacial values of $\delta^{18}\text{O}$ from our benthic stack to sea level elevation data from *Hearty and Kaufman* [2000] to see whether a linear relationship of $\delta^{18}\text{O}$ versus sea level exists for interglacial time, when the temperature effect is perhaps smaller [e.g., *Fairbanks and Matthews*, 1978].

[8] In another recent study, *Shackleton* [2000] concluded that global benthic $\delta^{18}\text{O}$ shows a significant temperature variation on the basis of the comparison of the relative strengths of the 41 kyr component in benthic $\delta^{18}\text{O}$ data from core V19-30 and that in the atmospheric $\delta^{18}\text{O}$ from the Vostok ice core. In that paper, a portion of the 41 kyr amplitude (that portion in core V19-30 that exceeds the atmospheric $\delta^{18}\text{O}$ in Vostok) is interpreted to reflect the global benthic temperature signal.

[9] We do not believe that the data support this interpretation by *Shackleton* [2000]. In Figure 1, we compare the amplitude of the 41 kyr peak in Vostok atmospheric $\delta^{18}\text{O}$ (tuned to 65°N summer insolation as suggested by *Petit et al.* [1999]), V19-30 benthic $\delta^{18}\text{O}$ (using the timescale of *Imbrie et al.* [1992]), and benthic $\delta^{18}\text{O}$ from nine records we analyze in this paper (based on our obliquity tuning described below). Each of these 11 records in Figure 1 has a different 41 kyr amplitude (amplitude is the modulus of the complex Fourier transform, taken using a boxcar window; zero padding is used to calculate intermediate frequencies); there is not a systematically larger obliquity response in benthic foraminifera than in Vostok atmospheric $\delta^{18}\text{O}$. Core V19-30 has a larger 41 kyr amplitude than do eight of the nine other benthic records, and Vostok has a 41 kyr amplitude higher than do four of the nine benthic cores. If we were to adopt Vostok as the accurate indicator of the changing isotopic content of the ocean, as suggested by *Shackleton* [2000], and if we were to attribute the rest of the obliquity amplitude of a benthic $\delta^{18}\text{O}$ record to the temperature of the deep ocean, we would have a different estimate of the benthic temperature signal for each core, including four with benthic warming, rather than cooling, during glacial periods. Thus we conclude that the benthic temperature estimate by *Shackleton* [2000] is core-specific and is not representative of the entire deep ocean.

[10] On a related matter, since the 41 kyr amplitude in core V19-30 is unusually large compared to the amplitude in other benthic

Table 1. Cores Examined in This Study

Core	Location	Water Depth, m	Average Sampling Interval, kyr	Average Sedimentation Rate, cm kyr^{-1}	References
DSDP 502	11°30'N, 79°23'W	3051	6.1	2.1 ^a	<i>deMenocal et al.</i> [1992]
DSDP 552	56°03'N, 23°14'W	2311	5.8	1.8	<i>Shackleton and Hall</i> [1984]
DSDP 607	41°00'N, 32°58'W	3427	3.6	4.1	<i>Ruddiman et al.</i> [1989]
ODP 659	18°05'N, 21°02'W	3070	4.1	3.1	<i>Tiedemann et al.</i> [1994]
ODP 664	00°06'N, 23°14'W	3806	3.4	3.6	<i>Raymo et al.</i> [1997]
ODP 677	01°12'N, 83°44'W	3461	2.7	3.9	<i>Shackleton and Hall</i> [1989]
ODP 846	03°06'S, 90°49'W	3307	2.7	3.7	<i>Mix et al.</i> [1995b]
ODP 849	00°11'N, 110°31'W	3851	3.7	2.8	<i>Mix et al.</i> [1995a]
ODP 925	04°12'N, 43°29'W	3040	2.3	3.6 ^a	<i>Bickert et al.</i> [1997]
ODP 927	5°28'N, 44°29'W	3326	3.3	4.3 ^a	<i>Bickert et al.</i> [1997]
ODP 980	55°29'N, 14°42'W	2179	0.7	10.9 ^a	<i>Flower et al.</i> [2000], <i>McManus et al.</i> [1999]
ODP 982	57°31'N, 15°53'W	1145	2.3	2.5	<i>Venz et al.</i> [1999]
TT013-PC72	00°07'N, 139°24'W	4298	3.2	1.7	<i>Murray et al.</i> [2000]

^a Sedimentation rates determined without tuning to obliquity (see text).

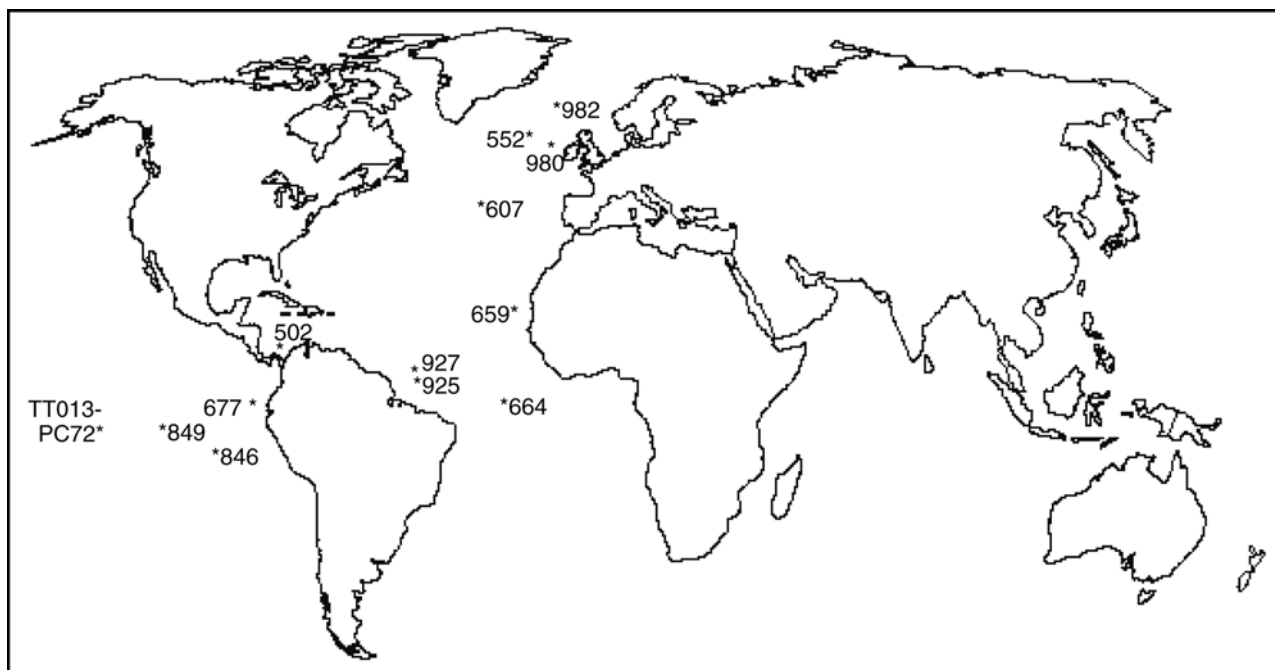


Figure 2. Locations of the cores used in this study. Information about each core is listed in Table 1.

$\delta^{18}\text{O}$ records, we suggest that the stack created by *Pisias et al.* [1984], which includes neighboring cores V19-28 and V19-29 in addition to V19-30, also does not represent the global signal. By contrast, the benthic stack created here, because it is an average of a larger number of longer records from more widely distributed sites, is designed to better approximate the true global signal.

[11] Here we assume that each record represents a different combination of global ice volume, benthic temperature, and local climatic and preservational effects. By taking a global average we hope to suppress these local effects, but we do not attempt to estimate the temperature component of the deep ocean. The stack we create is a record only of benthic $\delta^{18}\text{O}$, useful for climate modelers who may use this integrated signal to derive conclusions based on their own model assumptions.

3. Data and Methods

[12] Thirteen benthic $\delta^{18}\text{O}$ records were identified that each have sufficient duration and sampling frequency to study climate at

orbital frequencies. The cores considered for this study are listed in Table 1; sampling localities are shown in Figure 2. Supporting material, including the time series generated here, are available electronically.¹ The data are concentrated in three geographic regions: the North Atlantic, the tropical Atlantic, and the tropical Pacific Oceans. The cores were drilled at widely varying water depths, from 1145 m in the case of ODP Site 982 [*Venz et al.*, 1999] to 4298 m in the case of TT013-PC72 [*Murray et al.*, 2000]. For each record used in this study we have subtracted the mean value of $\delta^{18}\text{O}$ but have not normalized the variance. Subtracting the mean compensates for systematic offsets among the records, such as the sampling of isotopically different water masses or variation of temperature with depth but preserves the true magnitude of climate signals recorded at different locations.

[13] A critical task when constructing a composite stack is to establish a common timescale for the individual records prior to stacking. However, accurately determining the sedimentation rates for deep-sea cores has been a challenge. There are very few accurate radioisotopic decay systems that can be used to date sediment core material. Recent attempts to date aragonite sediment by U series methods [*Henderson and Slowey*, 2000] offer promise in this regard and perhaps will lead to more direct age determinations on sediment cores. Geomagnetic polarity stratigraphy is limited by the fact that there has been only one geomagnetic reversal in the last ~ 850 kyr. Radioisotopic ages of sea level highstand deposits, when applied to deep-sea core isotopic data, are among the most useful tie points for age determination. In the present paper, we take advantage of some new sea level highstand measurements by *Karner and Marra* [2002], who reassess the timing of the marine isotopic stage 11 sea level rise using dated volcanic horizons deposited in coastal onlap deposits of the Tiber River delta west of Rome.

Table 2. Depths of Preliminary Control Points^a

Core	Core Top (0 ka)	Termination II (135 ka)	Termination V (434 ka)	Centroid MIS 19 (790 ka)
DSDP 502	0	2.25	7.85	16.17
DSDP 552	0	2.46	6.96	14.11
DSDP 607	0	5.89	17.42	31.78
ODP 659	0	4.29	13.87	24.75
ODP 664	0	4.68	15.71	28.65
ODP 677	0	6.19	17.11	30.88
ODP 846	0	5.48	16.26	28.66
ODP 849	0	4.07	13.15	22.52
ODP 925	0	5.12	16.52	28.51
ODP 927	0	6.25	19.72	34.43
ODP 980	0	17.58	56.45	87.89
ODP 982	0	2.97	10.03	19.88
TT013-PC72	0	2.39	7.42	13.45

^a Depths are in meters.

¹Supporting material, including the time series generated here, are available electronically at World Data Center-A for Paleoclimatology, NOAA/NGDC, 325 Broadway, Boulder, CO 80303, USA (email: paleo@mail.ngdc.noaa.gov; URL: <http://www.ngdc.noaa.gov/paleo/data.html>)

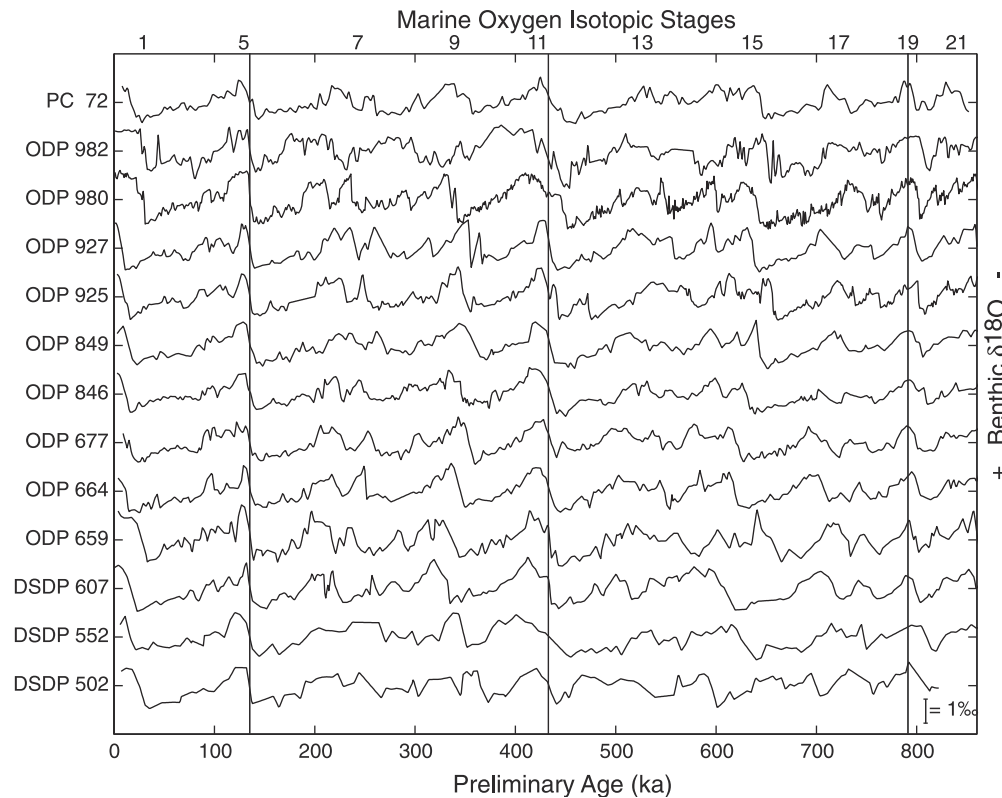


Figure 3. The 13 benthic $\delta^{18}\text{O}$ records with the radioisotopically determined (“untuned”) timescale. The control points used are shown with vertical lines and include the core top (0 ka), glacial Terminations II (135 ka) and V (434 ka), and the centroid of marine isotopic stage 19, set to the age of the Brunhes-Matuyama geomagnetic reversal (790 ka). The depths of these control points are listed in Table 2.

[14] The most frequently used alternative to radioisotopic dating is orbital tuning. In this process the timescale of the core (i.e., the relationship between depth and age) is adjusted to bring variations in isotopic data into agreement with calculated variations in the Earth’s orbital parameters. The major drawback of orbital tuning is that not all variations in the climate proxy are due to orbital changes, so there is a danger that variations will be misidentified. Alignment of misidentified data with an orbital target can exaggerate the perceived significance of the climatic response to orbital variations. Even a signal that consists entirely of random noise can be made to closely match orbital parameters [Neeman, 1993]. Muller and MacDonald [2000] give several examples from the paleoclimate literature of probable “overtuning” in which they argue that noise was orbitally tuned to match and artificially enhance agreement with the target model. Similarly, the graphic correlation method outlined by Prell *et al.* [1986] has the potential to exaggerate the amplitude of isotopic events since this process can lead to the alignment of noise in some cores with true isotopic events in other cores.

[15] In order to avoid overtuning we chose to use the 41 kyr obliquity cycle as the sole orbital tuning target. Obliquity appears to be a significant driving force in most benthic $\delta^{18}\text{O}$ records, with a signal-to-noise ratio that is relatively high when compared to that found from the precession signal. Therefore we have greater confidence that the 41 kyr signal in the data is a response to orbital forcing rather than noise. By avoiding use of the precession cycle in tuning we have the opportunity to study precession without the potential bias of artificially enhancing it. Additionally, the nature of the ~ 100 kyr cycle observed in many proxy records has been mysterious. Its amplitude is larger than that predicted in virtually all climate models (see reviews by Imbrie *et al.* [1993]

and Muller and MacDonald [2000]). In many models the strong 100 kyr climate cycle does not arise directly from eccentricity forcing but instead comes from a nonlinear response of climate to the envelope of the precession parameter [Imbrie and Imbrie, 1980]. Muller and MacDonald [1997] suggest the ~ 100 kyr cycle is better matched by variations in orbital inclination, the inclination angle of Earth’s orbital plane with respect to the invariable plane of the solar system. By using obliquity as the tuning target our results can be used to test the significance of climate response to precession forcing and also whether the ~ 100 kyr climate cycle is a better match to variations in eccentricity or orbital inclination.

[16] We established a preliminary timescale for each core by assigning radioisotopically determined ages to three $\delta^{18}\text{O}$ “control point” events. On the assumption that sedimentation continues at the present day and following the practice of the original authors of each record, depth 0 was assigned an age of 0 ka (see Table 2). The timing of glacial Termination II (marine isotopic stage 6.0) was set to 135 ka (representing an average of dates by Mesolella *et al.* [1969], Broecker and van Donk [1970], Winograd *et al.* [1997], and Henderson and Slowey [2000]). Termination V (marine isotopic stage 12.0) was set to 434 ka (based on interglacial highstand coastal deposits discussed by Karner and Marra [2002]). Mindful of the study by Tauxe *et al.* [1996], we initially set the Brunhes-Matuyama geomagnetic reversal to the centroid of marine isotopic stage 19, though we later make an allowance for the fact that in any given record, the reversal may be recorded several kiloyears before or after the centroid. We use the age of 790 ka for the reversal on the basis of the data of Singer and Pringle [1996], recalculated here to take into account the revised age of the Taylor Creek rhyolite standard as in the work of Renne *et al.* [1998]. Control point depths

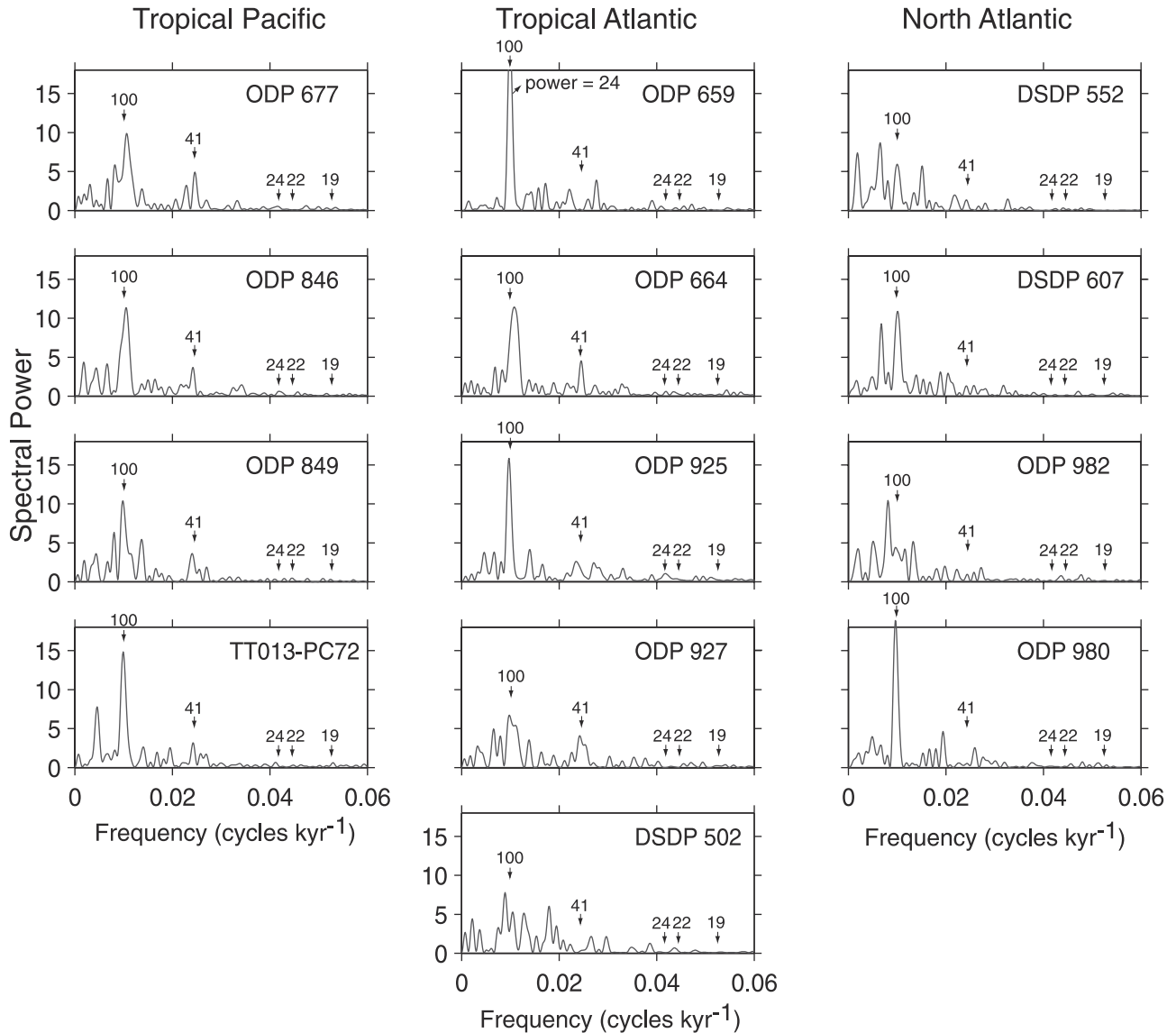


Figure 4. Power spectra of the 13 benthic $\delta^{18}\text{O}$ records with the untuned timescale. The left column includes cores from the tropical Pacific, the middle column includes cores from the tropical Atlantic, and the right column includes cores from the North Atlantic Ocean. The signal:noise of the spectral power near 0.01 cycles kyr^{-1} (100 kyr period) ranges from 8 (24:3) at ODP Site 659 to ~ 2 (8:4) at DSDP Site 502. We assess background noise in this paper based on the height of spectral peaks at nonorbital frequencies that are near the peaks of interest. Expected orbital frequencies are identified with arrows, with their corresponding periods in kiloyears.

for each core are listed in Table 2. Because there is uncertainty in the ages of each of these events, when we later applied orbital tuning, we relaxed the age constraints significantly to accommodate for these uncertainties (see section 4).

[17] Our initial timescale for each core was obtained by assuming constant sedimentation rates between each pair of control points. Because we use no radioisotopic age control older than the Brunhes-Matuyama geomagnetic reversal, the preliminary age scale beyond 790 ka is based on linear extrapolation and so becomes increasingly uncertain. We therefore truncated all cores by marine isotopic stage 22 (~ 850 ka). Figure 3 shows the benthic $\delta^{18}\text{O}$ records from the 13 cores with their untuned timescales. In most cases the data are taken from the benthic foraminifera species *Cibicoides wuellerstorfi*, but some records contain data from other *Cibicoides* species and from *Uvigerina*; species correction offsets (values used are from *Shackleton and*

Hall [1984]) were applied to these data either by the original researchers or by us (see original references in Table 1). Sedimentation rates resulting from this initial age model typically vary by $\sim 10\%$ from their mean value, though the sedimentation rate at ODP Site 980 varies by 19%.

4. Results and Discussion

[18] Figure 4 shows the power spectra of the 13 untuned cores; each power spectrum is normalized to unit mean (the power spectrum is the square of the Fourier transform using zero padding and a boxcar window). Note that the spectra are arranged in columns based on geographic location of the drill site. There are statistically significant peaks in many of the spectra at the frequency of 0.01 cycles kyr^{-1} (period 100 kyr), and most of the cores have excess

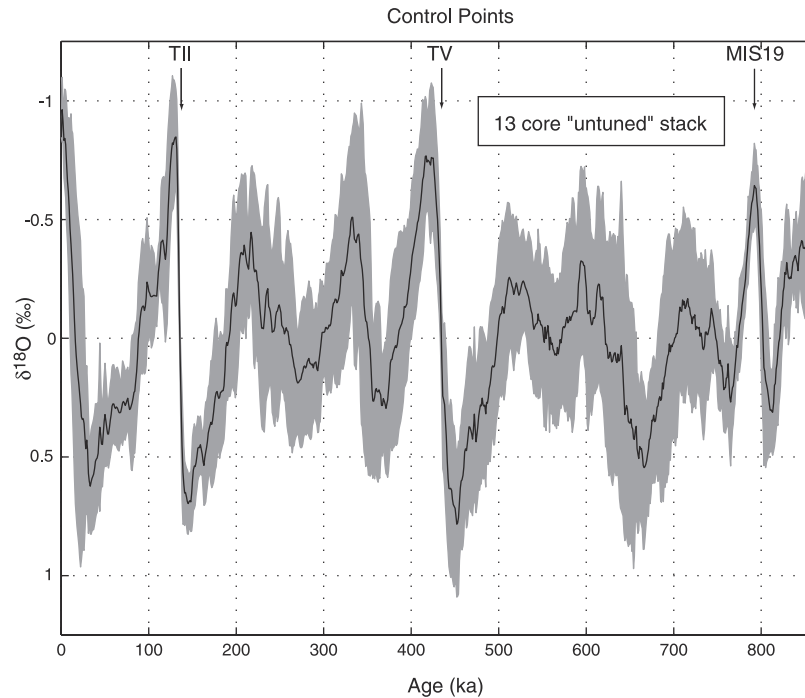


Figure 5. Stack (average value) of the 13 benthic $\delta^{18}\text{O}$ records with their untuned timescales and shown with the 1σ uncertainty envelope. The timescale for each core was based on radioisotopic ages of control points (identified with arrows at top of the plot) and assuming constant sedimentation between control points. TII and TV refer to glacial Terminations II and V, and MIS 19 refers to marine isotopic stage 19. The maximum sedimentation rate variation from the mean using these control point ages was 19% for ODP core 980; most cores had variations closer to $\pm 10\%$.

power in the vicinity of $0.024 \text{ cycles kyr}^{-1}$, corresponding to a period of 41 kyr.

[19] Figure 5 is the stack of these 13 cores that was composed using their untuned timescales. The uncertainty envelope represents the standard deviation of the 13 cores calculated at every kiloyear interval. The pattern for several of the cycles is very similar to the pattern seen in the planktic stacks mentioned above, with sharp terminations of glacial periods, brief interglacial peri-

ods, and a gradual onset of glaciation. Note that the widely described “saw-tooth shape” is clear in the periods 0–150 and 370–450 ka but is weak for the other cycles. The saw-tooth may be an artifact in that the sharpest terminations occur at our control points, at which all the cores are aligned. At other times, small variations in the sedimentation rate can cause the sudden terminations to appear to occur at different times, and this tends to blur the terminations into a more gradual shape.

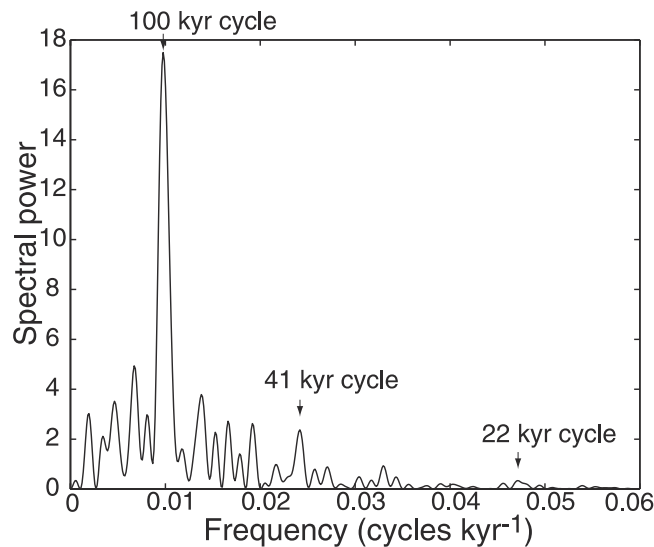


Figure 6. Power spectrum of the untuned stack. Expected orbital frequencies are identified with arrows, with their corresponding periods in kiloyears. The largest peak is centered at $0.01 \text{ cycles kyr}^{-1}$, with a period of 100 kyr. The full width at half the maximum power of this 100 kyr peak is $\Delta f/f = 0.13$.

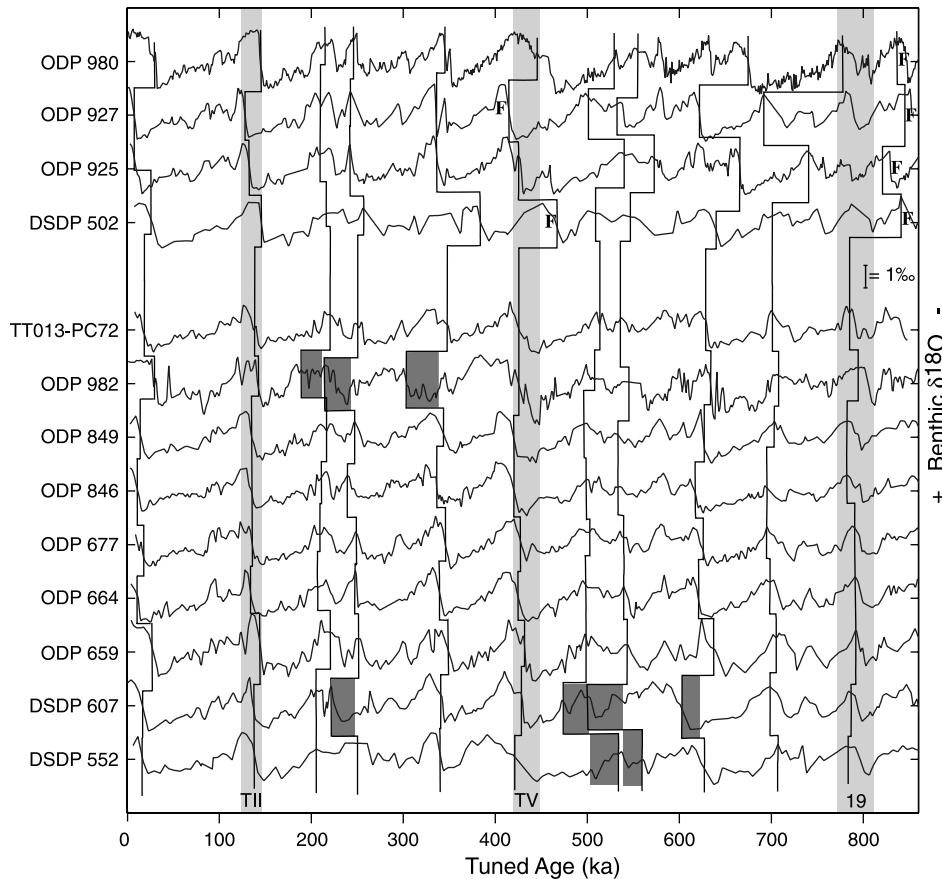


Figure 7. All 13 cores objectively tuned to obliquity (“minimally tuned”). Each core was tuned individually to the obliquity target, and the radioisotopic control points of Terminations II and V and marine isotopic stage 19 were permitted to slide, provided they remained within their 2σ radioisotopic age limits (limits shown with light gray bars). Vertical lines identify common isotopic events in the 13 cores. The upper four cores fail the filter test at radioisotopic control points labeled “F”. The lower nine cores pass the age control test at all radioisotopic control points. Shaded areas of cores DSDP 552, 607 and ODP 982 show where these three North Atlantic cores differ from the mean and often from each other by more than half an obliquity cycle, indicating inaccurate obliquity tuning. At no time does a tropical core that passed the filter test deviate from the mean by more than half an obliquity cycle, giving us confidence that the tuned timescale is accurate.

[20] Figure 6 shows the power spectrum of this 13-core untuned stack. The spectrum has peaks of high statistical significance (relative to local background) at $0.024 \text{ cycles kyr}^{-1}$ and $0.01 \text{ cycles kyr}^{-1}$, near those predicted by orbital theory. These results indicate that despite the absence of orbital tuning the untuned timescale is reasonably accurate. In particular, the spectrum is dominated by a single narrow peak at $0.01 \text{ cycles kyr}^{-1}$. Broecker and van Donk [1970] discovered the presence of the 100 kyr cycle, although its nature is still disputed. The narrowness of the 100 kyr peak ($\Delta f/f = 0.13$), particularly in untuned data, was cited as evidence for its astronomical origin [Muller and MacDonald, 1997].

[21] The presence of significant power in the vicinity of the expected obliquity peak (near $0.024 \text{ cycles kyr}^{-1}$) in Figure 6 suggests that obliquity tuning could be employed to improve the timescales of the individual cores. The $\sim 41 \text{ kyr}$ component of each record, based on the untuned timescale, was isolated with a Gaussian filter. An important issue was the selection of the correct bandwidth for this filter. We tried 39 different Gaussian filters, with bandwidth (root-mean-square deviations) from 8.66×10^{-4} to $6.35 \times 10^{-3} \text{ cycles kyr}^{-1}$. The former is comparable in width to the spectral peak of a pure 41 kyr sine wave of 850 kyr duration and so

is unable to accommodate much variation in sedimentation rate. The latter includes some frequencies closer to the expected precession and eccentricity/inclination frequencies than to the obliquity frequency and so is incautiously wide for obliquity tuning.

[22] A filter with a wide passband allows for more variability in sedimentation rate than does one with a narrow passband, but a wide filter also increases the likelihood that noise variations (those not associated with orbital changes) can be forced to match variations in the obliquity target. To limit such overtuning, we selected a passband that, for most of the cores, successfully produced obliquity-tuned ages that were consistent with the radioisotopic age limits of the control points. The age range we used for glacial Termination V (421–447 ka) included the systematic uncertainties inherent in $^{40}\text{Ar}/^{39}\text{Ar}$ dating, as discussed by Karner and Renne [1998], and the 95% confidence limit for this event as discussed by Karner and Marra [2002]. We permitted the age of Termination II to occur between 124 and 145 ka to encompass the dates of Mesolella *et al.* [1969], Broecker and van Donk [1970], Winograd *et al.* [1997], and Henderson and Slowey [2000]. The centroid of marine isotopic stage 19 was permitted to take an age between 770 ka and 810 ka, allowing for systematic and analytical

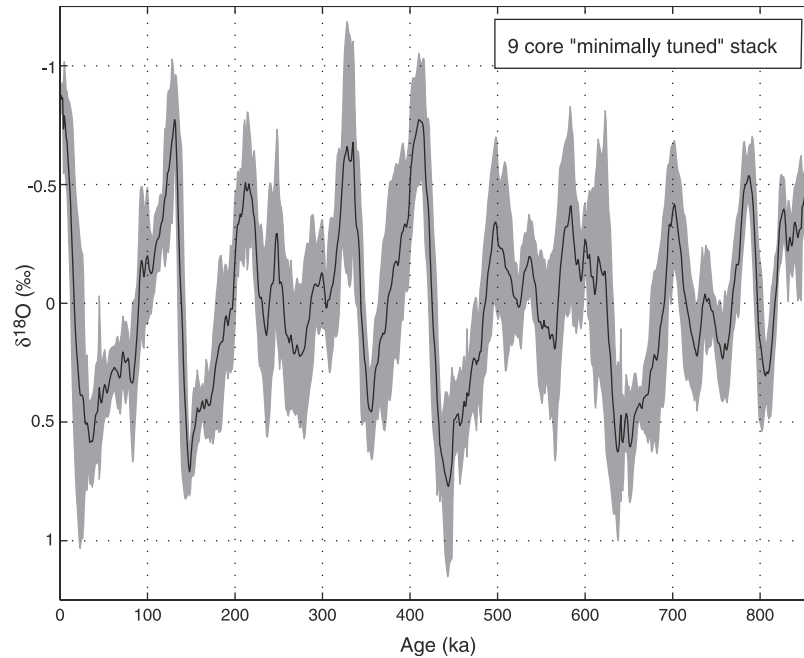


Figure 8. The minimally tuned benthic $\delta^{18}\text{O}$ stack of nine cores, with the 1σ uncertainty envelope.

uncertainties in the age of the Brunhes-Matuyama geomagnetic reversal and in the uncertainty in the precise correlation of the reversal event and the stage 19 centroid. We note that while based on radioisotopic data, the age limits that we have chosen for each control point are consistent with most orbitally based age scales that have been developed in the last decade [e.g., *Shackleton et al.*, 1990; *Bassinot et al.*, 1994; *Tauxe et al.*, 1996]. An additional uncertainty arises from the discrete sampling of the data in each core. To account for this uncertainty, half the spacing between measured data points was added to the uncertainty bracketing each control point age.

[23] The final choice of filter was one of intermediate width, with a relatively large number of cores that could be automatically tuned without adjusting the control point ages beyond their allowed uncertainties. The filter selected has a bandwidth (RMS) of 2.165×10^{-3} cycles kyr^{-1} and is centered on the obliquity frequency ($1/40.8$ cycles/ kyr^{-1}). We note, however, that the results we present here are not sensitive to this choice of filter width. Nearby filters produce stacks that are almost indistinguishable from the one we present here, and even the stacks produced from much wider filters, some of which include different cores, have identical timing for isotopic events. Tuning was accomplished using an automated program (written in the computer language Matlab) by applying the filter to both the individual core and to the obliquity signal. The computer program was written to find the maxima in the filtered isotopic data and assigned to these points the ages of the successive maxima in the filtered obliquity data. Thus there was an average of one tuning point every 41 kyr. Following this alignment procedure, a single-phase adjustment was made to return each core top age to 0 ka. Phase adjustments for the cores that passed the filter test varied from +5 kyr to -6 kyr, with three cores (ODP sites 659 and 982 and PC72) having negative values. The phase shift imposed to restore the core top ages to 0 ka seems to be unrelated to geographical location or water depth. This could indicate a flaw in our assumption of the core top age being 0 ka, or it could indicate unique phase lags at each site.

[24] All 13 records with the obliquity-tuned ages, including those that failed the filter test, are shown in Figure 7. Though

the ages of the radioisotopic control points were permitted to slide during the obliquity tuning (provided they stayed within their respective 2s age limits), there remains excellent alignment of marine isotopic stages 6.0, 12.0, and 19.1. Cores Deep Sea Drilling Program (DSDP) 502, ODP 925, ODP 927, and ODP 980 could not be automatically tuned with this filter; they yielded ages that were not consistent with the radioisotopic age limits (at positions “F” in Figure 7). In these four records, noise with periods near 41 kyr appears to cause objective obliquity tuning to fail. It might have been possible to hand-tune these cores to bring them into concordance with the cores that passed the filter test. Rather than introduce the possibility of bias, however, we chose to eliminate these cores from subsequent stacks. This seems a small price to pay, as nine records remain in our study, and the average of these should still suppress local variations more effectively than did previous stacks.

[25] A composite stack of the nine successfully obliquity-tuned cores was created by interpolating each record to 1 kyr intervals, then calculating the mean and standard deviation at every age point. This minimally tuned stack is shown in Figure 8. The uncertainty envelope in Figure 8 is narrower than was the envelope of the untuned stack, indicating that obliquity tuning has improved the alignment of isotopic events. The 1σ uncertainty envelope of the untuned stack had a mean width of 0.31‰; the nine-core minimally tuned stack has a mean width of its 1σ uncertainty envelope of 0.27‰. Figure 9 shows the power spectrum of the minimally tuned stack. The largest difference between this spectrum and that of the untuned stack is the dramatic enhancement of the 41 kyr peak. Of course, obliquity tuning would create such a peak even from random noise; the true obliquity response is probably somewhat less than depicted in Figure 9. As with the untuned stack, the minimally tuned stack has a significant peak near 0.01 cycles kyr^{-1} . This ~ 100 kyr peak has a full width at half the maximum power of $\delta f/f = 0.14$, comparable to that in the power spectrum of the untuned stack. Two peaks near the precession frequencies of 0.0425, 0.0446, and 0.0529 cycles kyr^{-1} are higher with respect to the local background than they are in the untuned stack (Figure 6). However, only one of the peaks actually coincides

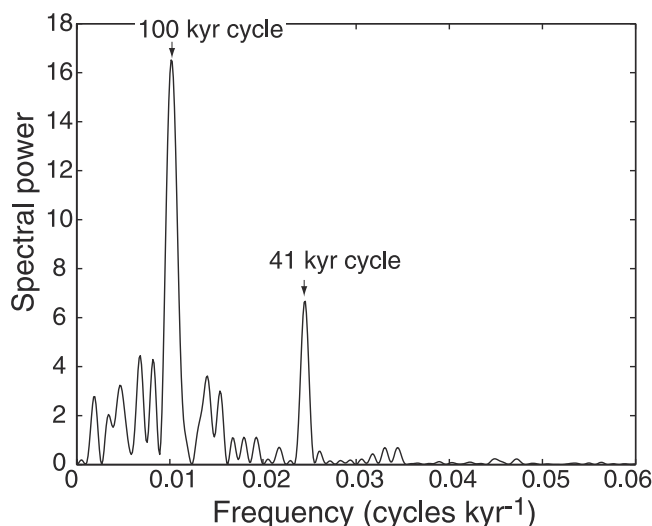


Figure 9. Power spectrum of the minimally tuned stack. Largest peaks are centered at ~ 0.01 cycles kyr^{-1} (full width at half the maximum power is $\Delta f/f = 0.14$) and 0.024 cycles kyr^{-1} . The latter peak is a necessary product of obliquity tuning.

with precession (0.0446 cycles kyr^{-1}). The other equally high peak is several times its own width from true precession frequencies and so is probably not a precession peak.

[26] Because our tuning procedure made adjustments to filtered data with periods already close to 41 kyr, derived sedimentation rates did not change by more than $\pm 35\%$ from the mean value for any of the cores. The RMS deviation from mean value of the sedimentation rates for the nine benthic stack cores averaged 9.5% . This seems physically more plausible than sedimentation rates required to construct the SPECMAP stack [Imbrie *et al.*, 1984], whose RMS deviation from mean values averaged 58.4% and exceeded $\pm 300\%$ in some places [see Muller and MacDonald, 2000].

[27] As an alternative to simple averaging of the cores' isotopic data, we examined the nine records with empirical orthogonal function (EOF) analysis [see Peixoto and Oort, 1992]. Each EOF is a linear combination of the nine records chosen in such a way as to be completely uncorrelated with all other EOFs and with the variance of the system concentrated in as few EOFs as possible. Having done this, we found that the principal component of the EOF analysis is virtually indistinguishable from the stack created by averaging, and it accounts for 59% of the variance of the nine-core system.

4.1. Other Orbital Signals in the Minimally Tuned Stack

[28] Because the nine-core stack is minimally tuned to a target containing only obliquity, we can use this stack to study other orbital cycles in the data. In the power spectrum of the minimally tuned stack (Figure 9) the dominant feature is the single narrow peak at 0.01 cycles kyr^{-1} , corresponding to a period of 100 kyr. We note that this peak was present using the untuned timescale. The presence of spectral power in the 100 kyr region is well known and is usually attributed to variations in the Earth's orbital eccentricity (see, for example, the review by Imbrie *et al.* [1993]). However, Muller and MacDonald [1997, 2000] drew attention to the narrow width of this peak, as observed in the analysis of many planktic and benthic data sets as well as in prior stacks. The shape of the peak in the present stack agrees with that reported by them and is inconsistent with the triplet of peaks expected if the variation were driven by eccentricity.

[29] In Figure 9, the statistical significance of peaks at expected precession frequencies is marginal. The entire frequency range

0.04 – 0.06 cycles kyr^{-1} , which might loosely be called the precession band, contains only 1.7% of the total variance of the nine-core stack. To be sure that we have not missed the precession response by tuning to obliquity and to place an upper limit on the benthic $\delta^{18}\text{O}$ response to precession forcing, we conducted several tests. First, starting with the obliquity-tuned timescale, we applied a band-pass filter to isolate and tune the precession signal (the band-pass filter was wide enough to include the 24 and 22 kyr doublet). After aligning core top ages to 0 ka and stacking again, the variance in the precession band was 3.2% . Because this is based on precession tuning, Figure 9 is an appropriate benchmark only if there is, a priori, a reason to believe that the response to

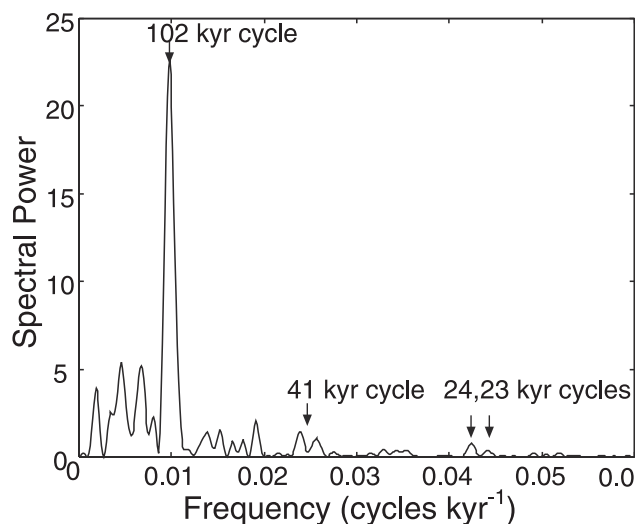


Figure 10. Power spectrum of the precession-tuned nine-core stack. The largest peak is centered at ~ 0.01 cycles kyr^{-1} . The precession frequencies are expected at 0.042 and 0.045 cycles kyr^{-1} . Obliquity, at 0.024 cycles kyr^{-1} , does not improve substantially relative to the power exhibited in the untuned stack (see Figure 6). This plot shows that objectively tuning to precession does not yield an accurate timescale.

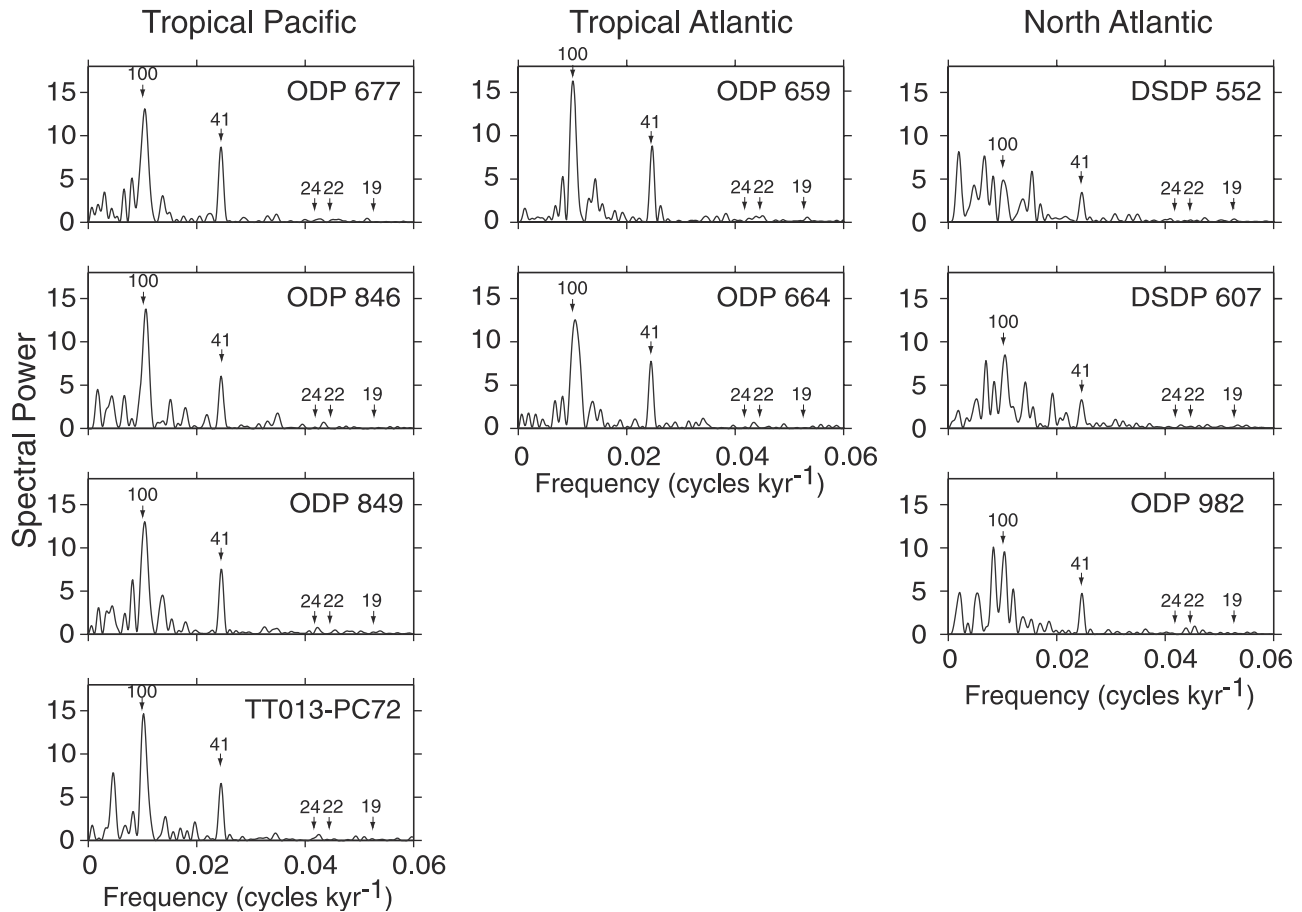


Figure 11. Power spectra of the nine individual cores with timescales determined by obliquity tuning. Comparison with Figure 4 shows greatly enhanced components with periods of 41 kyr, the result of tuning to obliquity. As in Figure 4, the left column includes cores from the tropical Pacific, the middle column includes cores from the tropical Atlantic, and the right column includes cores from the North Atlantic Ocean. Expected orbital frequencies are identified with arrows, with their corresponding periods in cycles per kiloyear. Note that the North Atlantic cores lack the single narrow 100 kyr peak characteristic of all the other records.

precession stands out above background, so that it makes a suitable tuning target. With wider filters, designed to include the 24, 22, and 19 kyr precession peaks, only one core (ODP Site 659) passed our consistency test with the radioisotopic control point ages.

[30] As a second test we started with the untuned timescale and used precession as the sole tuning target. After adjusting core top ages to 0 ka, tuning to precession alone increased the spectral power in the precession band to 3.8% of the total variance (Figure 10). As a test of the accuracy of the precession tuning, we checked the significance of the obliquity peak in the precession-tuned stack. A precession-tuned timescale, if valid, should produce an obliquity peak because adjusting the timescale to align every ~ 20 kyr “precession” peak guarantees that the timescale will also be correct on the scale of 41 kyr. However, the power spectrum of the precession-tuned stack in Figure 10 has a split obliquity peak, with peak power comparable to that at nearby nonastronomical frequencies. This suggests that the process of tuning to precession produced an inaccurate timescale for some of the cores, probably because noise near precession frequencies was tuned to match the precession target. If so, the upper limit of 3.8% of the variance in the precession band may be higher than the true response to precession forcing.

[31] As a third exercise, we repeated the precession tuning, this time relaxing the assumption that every core top has an age of 0 ka,

and instead, we aligned the precession response in each record. In this stack the presumed precession signal in each core is made to add constructively. This would be an appropriate stack to consider only if the following are true: (1) there is an a priori reason to believe that the precession response has a high enough signal:noise ratio to be useful in tuning, (2) the response to precession is globally synchronous, and (3) the top of a sediment core may have any age up to ~ 23 kyr. The stack constructed in this manner had 8.0% of the variance in the precession band. Once again, the spectral peak corresponding to obliquity was split, with peak power only at the background level, indicating that the timescale generated by objectively tuning benthic $\delta^{18}\text{O}$ to precession is inaccurate. The figure of 8.0% of the variance being in the precession band is thus likely to be overestimated.

[32] As a final check on the role of precession forcing of benthic $\delta^{18}\text{O}$, we performed Monte Carlo simulations to see whether tuning to obliquity alone ought to be sufficient to bring out ~ 20 kyr peaks if they were truly present in the signal. The simulations showed that precession peaks are suppressed proportionately to the amount of variability in the sedimentation rate. For a precession peak to fall by a factor of 2 in spectral power, sedimentation would have to vary routinely by $>100\%$ within a single obliquity cycle. Since, over timescales from hundreds of kiloyears down to 40 kyr, our sedimentation rates derived by obliquity tuning vary by less than $\pm 35\%$,

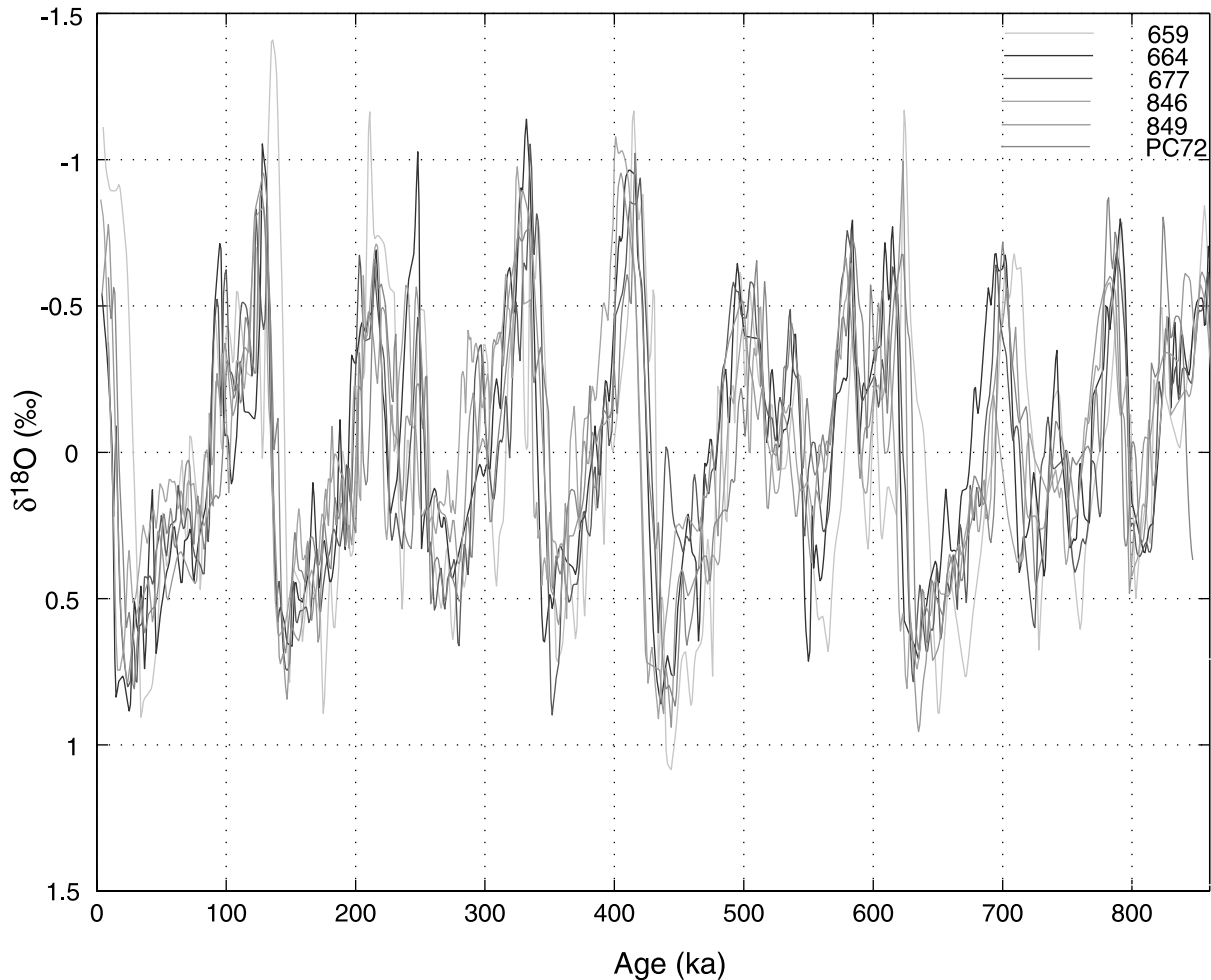


Figure 12. The six obliquity-tuned records from tropical latitudes. These are ODP Sites 659, 664, 677, 846, and 849 and core TT013-PC72. The mean has been subtracted from each, but the amplitudes have not been adjusted. Therefore the spread in the data reflects the true variation in $\delta^{18}\text{O}$ at the seven drilling sites. See color version of this figure at back of this issue.

with RMS deviations of $\sim 10\%$, it seems unreasonable to assume variations in sedimentation of 100% occur on the 20 kyr scale. It is therefore unlikely that precession is suppressed by more than a factor of 2, which is consistent with the upper limit of 3–4% of the total variance being in the precession band that we obtained above.

[33] We do not conclude that the precession response in the benthic $\delta^{18}\text{O}$ record is absent but only that it is not significantly stronger than other background fluctuations in the same band, and therefore it provides a poor tuning target for the benthic $\delta^{18}\text{O}$ records. In contrast, the pacemaker [Hays *et al.*, 1976], SPECMAP [Imbrie *et al.*, 1984], and low latitude [Bassinot *et al.*, 1994] stacks have relatively high spectral peaks at precession frequencies, with 9.0, 12.3, and 11.3% of the variance, respectively, in the frequency range 0.04–0.06 cycles kyr^{-1} . The difference between these stacks and the benthic stack created here could arise from the fact that they used planktic, rather than benthic, $\delta^{18}\text{O}$. These two proxies need not be recording the same aspects of climate and so need not be identical. It is also possible that overtuning artificially enhanced the strong precession signals in these prior stacks since the precession signal was part of the target model used in each of these studies.

[34] The composite benthic record of Piasias *et al.* [1984] is a study of $\delta^{18}\text{O}$ as a function of depth in core V19-29 rather than age.

If constant sedimentation is assumed for V19-29, then 11% of the variance is in the frequency range 0.04–0.06 cycles kyr^{-1} . If, however, the Piasias *et al.* stack is correlated with the SPECMAP stack, then 18% of the variance is in the precession band. The high variance in the precession band in the Piasias *et al.* [1984] stack contrasts with the low precession signal that we see in our stacks. It is possible that the stronger precession they see is a combined effect of local climate conditions and possible overtuning of the SPECMAP record. The “noise” seen in benthic signals could represent real climate variations that are not due to precession. Such noise would then be identical in disparate records. If one record were overtuned, then any other record that was correlated with it would also be overtuned, in the sense that fluctuations not associated with precession would be forced to be in phase with it. As we noted above, the Piasias *et al.* stack is composed of three cores from the same part of the Pacific Ocean, and the precession response recorded there may simply be higher than the global average.

[35] The weakness of precession in $\delta^{18}\text{O}$ signals has previously been noted by Karner and Muller [1999; see also Muller and MacDonald, 2000] who noted it in a record (ODP Site 659) that simultaneously showed a strong precession signal in wind-blown dust, which is a proxy for Saharan aridity. They concluded that the

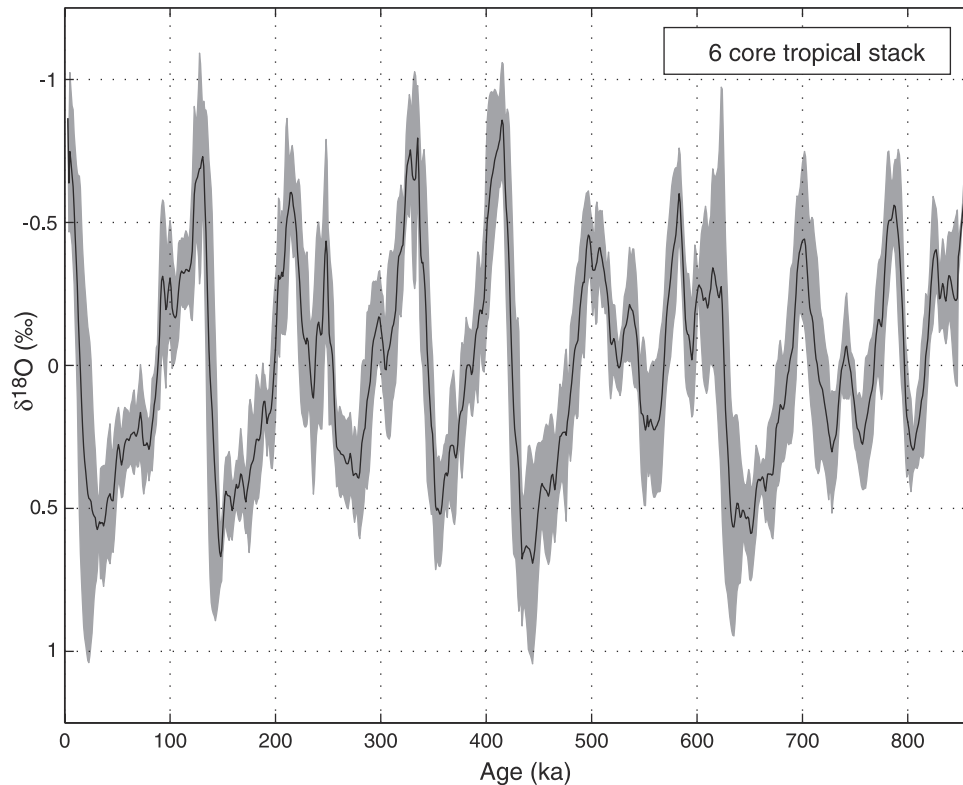


Figure 13. Stack of the six obliquity-tuned tropical benthic $\delta^{18}\text{O}$ records, with the 1σ uncertainty envelope.

dust was likely a response to local equatorial climate driven by insolation but that the $\delta^{18}\text{O}$ record was responding primarily to the 100 kyr climate oscillation.

4.2. Support for a Tropical Stack

[36] We now depart from our “hands off” approach to consider whether the stack could be improved by omitting several cores. Figure 11 shows the obliquity-tuned spectrum of each core, arranged by geographical region. Note that the narrow 100 kyr peak, the largest feature in untuned benthic $\delta^{18}\text{O}$ records (Figure 4), is more diffuse in the obliquity-tuned spectra of the North Atlantic cores. In contrast, the tropical data from both the Atlantic and Pacific have better core-to-core agreement, with well-defined 100 kyr spectral peaks. From this observation we conclude that the objective obliquity tuning applied to the North Atlantic cores was less successful than was the tuning applied to the tropical records. This may be a consequence of more variable sedimentation rates in the North Atlantic Ocean plus higher levels of background noise in these data, perhaps due to close proximity to glacial meltwater and ice discharge areas. For these North Atlantic cores we believe that a better timescale could be determined through hands-on tuning; we prefer not to do this here because of the subjectivity it would introduce.

[37] An examination of the individual cores shows the apparent failures of the automated tuning process. In particular, we have identified locations where we believe that the strict computerized tuning process introduced errors of greater than half an obliquity cycle, and these are identified with shaded boxes on the North Atlantic cores in Figure 7. Because these comparisons suggest that it is not possible to construct a reasonable timescale for the three North Atlantic cores by our objective methods, we create an alternative stack using only tropical cores. If we were to adjust the North Atlantic timescales by the graphic correlation method to

make the peaks agree with those of the tropical data, as suggested by the vertical lines in Figure 7, then the disagreement could be eliminated. However, for the present exercise we have not forced the alignment of any isotopic features; we have chosen to avoid introducing this type of subjectivity. We plot the six tropical cores together in Figure 12 to show that the tropical $\delta^{18}\text{O}$ signal is easily traced from one core to the next. In Figure 12 the mean was subtracted from each record, but the records were not normalized to unit variance. Therefore Figure 12 shows the true variations in $\delta^{18}\text{O}$ for each core. Figure 13 is the tropical stack created using the six obliquity-tuned tropical cores. The uncertainty envelope of the tropical stack is much narrower than that of the nine-core stack (0.22‰ for the six-core stack versus 0.27‰ for the nine-core stack), but the mean values of the tropical stack differ only slightly from those of the nine-core minimally tuned stack. The power spectrum of the tropical stack is in Figure 14. Again, there is a narrow peak near 100 kyr, with full width at half the maximum power is $\Delta f/f = 0.15$.

4.3. Comparison With Terrace Elevation Data

[38] In Figure 15 we compare the tropical stack with the elevations of sea level highstands, estimated by *Hearty and Kaufman* [2000] from a study of coral terraces in the Bahamas. By considering sea level highstands only, we are comparing the relationship between interglacial minima in $\delta^{18}\text{O}$ with the minima in global ice volume. We make a linear approximation between these two records from sea level highstands of marine isotopic stages 1, 5, 7, 9, 11, and 13. The best fit straight line between $\delta^{18}\text{O}$ at peak interglacial conditions and sea level highstand elevations is given by $\delta^{18}\text{O} (\text{‰}) = 0.014 \times \text{sea level (m)} + 0.67$. This line yields agreement between benthic $\delta^{18}\text{O}$ and sea level for each of the last six interglacial periods at better than the 1s level; the largest disagreement is approximately 6 m, or $\sim 0.1\%$. We note that

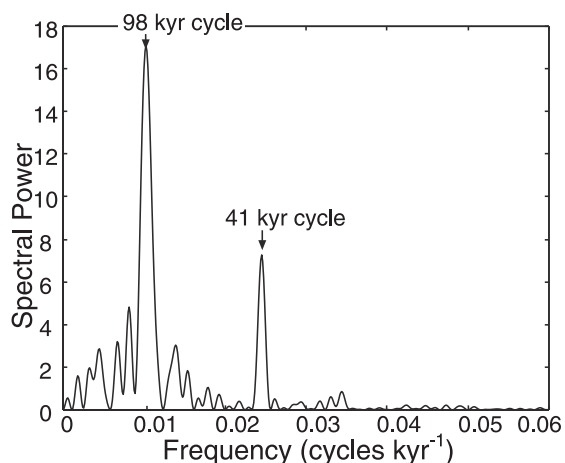


Figure 14. Power spectrum of the tropical stack. The largest peak is at ~ 0.01 cycles kyr^{-1} .

different assumptions about whether $\delta^{18}\text{O}$ reflects only global ice volume or a combination of global ice volume and temperature do not affect this estimate; whatever fraction of the $\delta^{18}\text{O}$ variations is due to temperature changes, the benthic foram $\delta^{18}\text{O}$ record is nevertheless a good sea level indicator. Only the value of the proportionality constant is sensitive to the different interpretations of the $\delta^{18}\text{O}$ signal.

[39] The measurements of glacio-eustatic sea level are certainly indicators of global conditions; the tropical benthic stack was constructed from records that probably contained both global and local influences. We believe that the slight disagreement between the $\delta^{18}\text{O}$ stack and the terrace elevation data is due to local variability which remains in the tropical stack, and we estimate that this local variability is responsible for roughly 0.1‰ out of a total glacial-interglacial amplitude of 1.3‰. In this way, we conclude that local climate effects may be responsible for $\sim 10\%$ of the variance of the tropical stack; the remaining $\sim 90\%$ are probably a true reflection of global climate. This figure is necessarily approximate because there is no guarantee that the relationship between foraminiferal $\delta^{18}\text{O}$ and sea level is exactly linear.

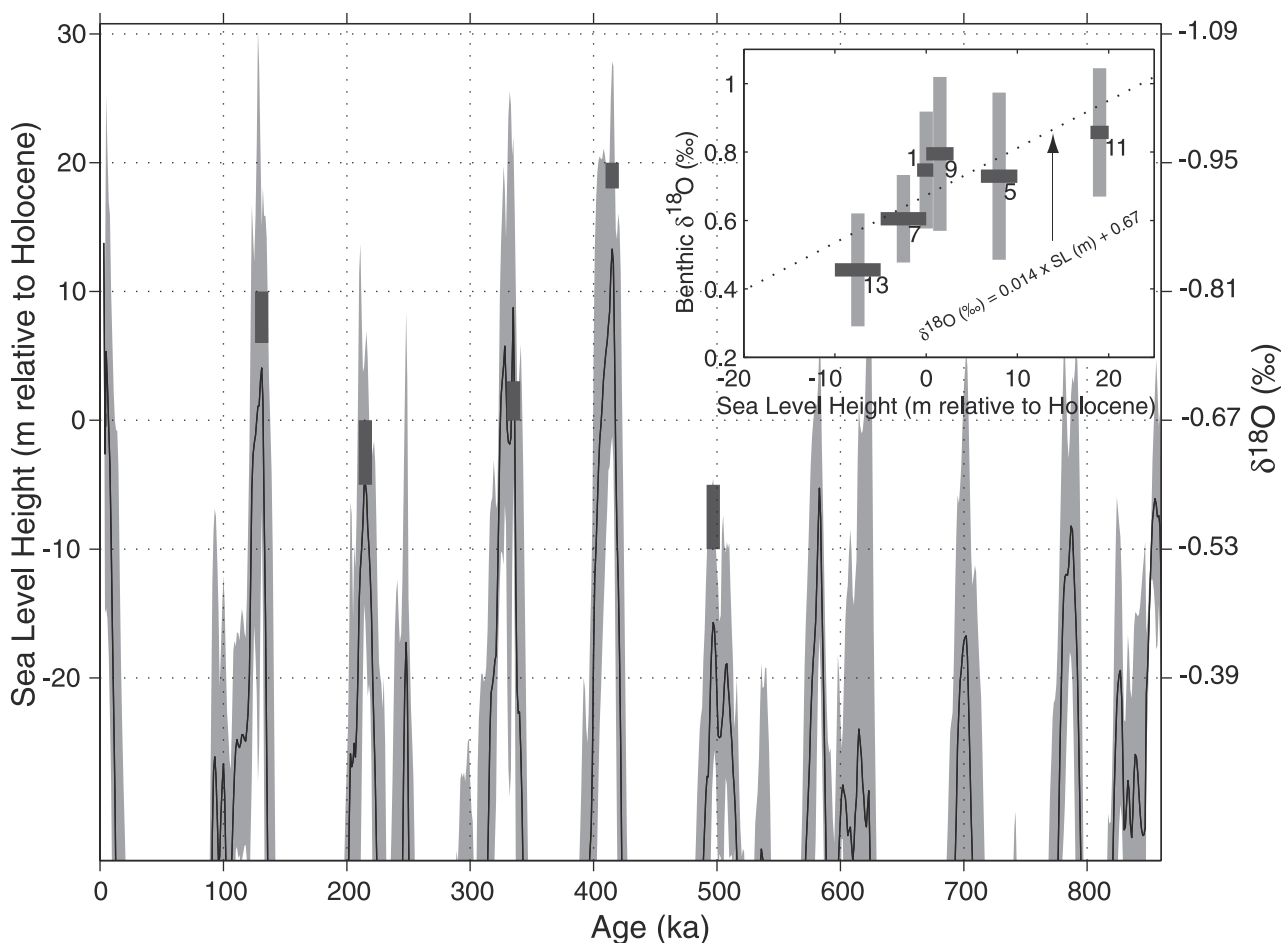


Figure 15. Comparison of $\delta^{18}\text{O}$ from the tropical stack at peak interglacial conditions with coral terrace elevation data from *Hearty and Kaufman* [2000]. Inset shows the best fit line of interglacial sea level versus $\delta^{18}\text{O}$ for marine isotopic stages 1, 5, 7, 9, 11, and 13. Error limits for each isotopic stage are based on the error envelope of the tropical stack and the elevation ranges reported by *Hearty and Kaufman* [2000]. The regression line suggests a shift of 0.014‰ in $\delta^{18}\text{O}$ m^{-1} in sea level. The large error envelope of the $\delta^{18}\text{O}$ data precludes us from estimating interglacial sea level heights to any better than ~ 10 m.

5. Conclusions

[40] The benthic stacks that we have constructed were produced with minimal tuning and a “hands off” approach to avoid bias. They offer a direct assessment of climate preserved in the deep ocean for the last ~850 kyr. The large number of records incorporated into these stacks offers hope that they could give a true global average, with minimal contributions from regional effects.

[41] The untuned 13-core stack shows many features in basic agreement with the previously constructed planktic stacks. They all show the presence of a single, narrow 100 kyr spectral peak which dominates the $\delta^{18}\text{O}$ record of the last ~850 kyr. In the obliquity-tuned stack we found that even allowing for rapid variations in sedimentation rate, precession accounts for probably no more than 3–4% of the variance in the record. This is a lower estimate of the significance of precession than in previously published planktic and benthic stacks. To reconcile these differences, either the prior records reflect climate signals which are surface effects or non-global effects, or they are affected by overtuning. Alternatively, variations in the sedimentation rate large enough to suppress precession by more than a factor of two may exist in our time-scales, though we think this is unlikely for most cores.

[42] The objective tuning technique we employed produces more satisfactory results for tropical cores than for North Atlantic ones. This seems to be due to large sedimentation rate variations in the North Atlantic, which limited our ability to tune them objectively. The removal of these North Atlantic cores to create the six-core tropical stack may bias the tropical stack toward an Antarctic bottom water signal, but we note that there is little difference between the stacks that we created including or excluding these three North Atlantic cores. The tropical stack provides estimates of interglacial sea level that agree with coral terrace data, and the obliquity-tuned timescale imposes sedimentation rates that seem more physically plausible than those used to construct the planktic stacks. We suggest that this stack will be a useful template for global climate.

[43] **Acknowledgments.** We are grateful to Ellen Thomas, Tim Herbert, and Lisa Sloan for their constructive reviews of this manuscript. This work was supported in part by the Office of Biological and Environmental Research of the U.S. Department of Energy, under grant DE-FG03-97ER62467. Jonathan Levine thanks the William and Flora Hewlett Foundation for a graduate research fellowship. Richard Muller thanks the Ann and Gordon Getty Foundation and the Folger Foundation for their support.

References

- Bassinot, F. C., L. D. Labeyrie, E. Vincent, X. Quidelleur, N. J. Shackleton, and Y. Lancelot, The astronomical theory of climate and the age of the Brunhes-Matuyama magnetic reversal, *Earth Planet. Sci. Lett.*, *126*, 91–108, 1994.
- Beck, J. W., J. Recy, F. Taylor, R. L. Edwards, and G. Cabioch, Abrupt changes in early Holocene tropical sea surface temperature derived from coral records, *Nature*, *385*, 705–707, 1997.
- Bickert, T., W. B. Curry, and G. Wefer, Late Pliocene to Holocene (2.6–0 Ma) western equatorial Atlantic deep-water circulation: Inferences from benthic stable isotopes, *Proc. Ocean Drill. Program Sci. Results*, *154*, 239–253, 1997.
- Broecker, W. S., *The Glacial World According to Wally*, Lamont-Doherty Earth Obs., Palisades, N. Y., 1995.
- Broecker, W. S., and J. van Donk, Insolation changes, ice volumes, and the ^{18}O record in deep-sea cores, *Rev. Geophys.*, *8*, 169–197, 1970.
- Chappell, J., and N. J. Shackleton, Oxygen isotopes and sea level, *Nature*, *324*, 137–140, 1986.
- deMenocal, P. B., D. W. Oppo, R. G. Fairbanks, and W. L. Prell, Pleistocene $\delta^{13}\text{C}$ variability of North Atlantic intermediate water, *Paleoceanography*, *7*, 229–250, 1992.
- Elderfield, H., and G. Ganssen, Past temperature and $\delta^{18}\text{O}$ of surface ocean waters inferred from foraminiferal Mg/Ca ratios, *Nature*, *405*, 442–445, 2000.
- Fairbanks, R. G., and R. K. Matthews, The marine oxygen isotope record in Pleistocene coral, Barbados, West Indies, *Quat. Res.*, *10*, 181–196, 1978.
- Flower, B. P., D. W. Oppo, J. F. McManus, K. A. Venz, D. A. Hodell, and J. L. Cullen, North Atlantic intermediate to deep water circulation and chemical stratification during the past 1 Myr, *Paleoceanography*, *15*, 388–403, 2000.
- Hastings, D. W., A. D. Russell, and S. R. Emerson, Foraminiferal magnesium in *Globigerinoides sacculifer* as a paleotemperature proxy, *Paleoceanography*, *13*, 161–169, 1998.
- Hays, J. D., J. Imbrie, and N. J. Shackleton, Variations in the Earth's orbit: Pacemaker of the Ice Ages, *Science*, *194*, 1121–1132, 1976.
- Hearty, P. J., and D. S. Kaufman, Whole-rock aminostratigraphy and Quaternary sea-level history of the Bahamas, *Quat. Res.*, *54*, 163–173, 2000.
- Henderson, G. M., and N. C. Slowey, Evidence from U-Th dating against Northern Hemisphere forcing of the penultimate deglaciation, *Nature*, *404*, 61–65, 2000.
- Imbrie, J., and J. Z. Imbrie, Modeling the climatic response to orbital variations, *Science*, *207*, 943–952, 1980.
- Imbrie, J., J. D. Hays, D. G. Martinson, A. McIntyre, A. C. Mix, J. J. Morley, N. G. Pisias, W. L. Prell, and N. J. Shackleton, The orbital theory of Pleistocene climate: Support from a revised chronology of the marine $\delta^{18}\text{O}$ record, in *Milankovitch and Climate*, part 1, edited by A. Berger, pp. 269–305, D. Reidel, Norwell, Mass., 1984.
- Imbrie, J., et al., On the structure and origin of major glaciation cycles, 1, Linear responses to Milankovitch forcing, *Paleoceanography*, *7*, 701–738, 1992.
- Imbrie, J., et al., On the structure and origin of major glaciation cycles, 2, The 100,000 year cycle, *Paleoceanography*, *8*, 699–735, 1993.
- Karner, D. B., and F. Marra, $^{40}\text{Ar}/^{39}\text{Ar}$ dating of glacial Termination V and the duration of marine isotopic stage 11, in *Marine Isotopic Stage 11: An Extreme Interglacial?*, *Geophys. Monograph Ser.*, edited by A. Droxler, R. Poore, L. Burckle, L. Osterman, AGU, Washington, D. C., in press, 2002.
- Karner, D. B., and R. A. Muller, The weakness of precession in global ice volume records, *Rep. 44777*, Lawrence Berkeley Natl. Lab., Berkeley, Calif., 1999.
- Karner, D. B., and P. R. Renne, $^{40}\text{Ar}/^{39}\text{Ar}$ geochronology of Roman volcanic province tephra in the Tiber River valley: Age calibration of middle Pleistocene sea-level changes, *Geol. Soc. Am. Bull.*, *110*, 740–747, 1998.
- Lea, D. W., D. K. Pak, and H. J. Spero, Climate impact of late Quaternary equatorial Pacific sea surface temperature variations, *Science*, *289*, 1719–1724, 2000.
- Mashiotta, T. A., D. W. Lea, and H. J. Spero, Glacial-interglacial changes in subantarctic sea surface temperature and $\delta^{18}\text{O}$ -water using foraminiferal Mg, *Earth Planet. Sci. Lett.*, *170*, 417–432, 1999.
- McManus, J. F., D. W. Oppo, and J. L. Cullen, A 0.5-million-year record of millennial-scale climate variability in the North Atlantic, *Science*, *283*, 971–975, 1999.
- Mesolella, K. J., R. K. Matthews, W. S. Broecker, and D. L. Thurber, The astronomical theory of climatic change: Barbados data, *J. Geol.*, *77*, 250–274, 1969.
- Mix, A. C., N. G. Pisias, W. Rugh, J. Wilson, A. Morey, and T. K. Hagelberg, Benthic foraminifer stable isotope record from site 849 (0–5 Ma): Local and global climate changes, *Proc. Ocean Drill. Program Sci. Results*, *138*, 371–412, 1995a.
- Mix, A. C., J. Le, and N. J. Shackleton, Benthic foraminifera stable isotope stratigraphy of site 846: 0–1.8 Ma, *Proc. Ocean Drill. Program Sci. Results*, *138*, 839–854, 1995b.
- Muller, R. A., and G. J. MacDonald, Glacial cycles and astronomical forcing, *Science*, *277*, 215–218, 1997.
- Muller, R. A., and G. J. MacDonald, *Ice Ages and Astronomical Causes: Data, Spectral Analysis and Mechanisms*, Springer-Verlag, New York, 2000.
- Murray, R. W., C. Knowlton, M. Leinen, A. C. Mix, and C. H. Polsky, Export production and carbonate dissolution in the central equatorial Pacific Ocean over the past 1 Myr, *Paleoceanography*, *15*, 570–592, 2000.
- Neeman, B., Orbital tuning of paleoclimate records: A reassessment, *Rep. LBNL-39572*, Lawrence Berkeley Natl. Lab., Berkeley, Calif., 1993.
- Petit, J. R., et al., Climate and atmospheric history of the past 420,000 years from the Vostok ice core, Antarctica, *Nature*, *399*, 429–436, 1999.
- Peixoto, J. P., and A. H. Oort, *Physics of Climate*, Am. Inst. of Phys., College Park, Md., 1992.

- Pisias, N. G., D. G. Martinson, T. C. Moore, N. J. Shackleton, W. Prell, J. D. Hays, and G. Boden, High resolution stratigraphic correlation of benthic oxygen isotopic records spanning the last 300,000 years, *Mar. Geol.*, *56*, 119–136, 1984.
- Prell, W. L., J. Imbrie, D. G. Martinson, J. J. Morley, N. G. Pisias, N. J. Shackleton, and H. F. Streeter, Graphic correlation of oxygen isotope stratigraphy application to the late Quaternary, *Paleoceanography*, *1*, 137–162, 1986.
- Raymo, M. E., D. W. Oppo, and W. Curry, The mid-Pleistocene climate transition: A deep sea carbon isotopic perspective, *Paleoceanography*, *12*, 546–559, 1997.
- Renne, P. R., C. C. Swisher, A. L. Deino, D. B. Karner, T. L. Owens, and D. J. DePaolo, Inter-calibration of standards, absolute ages and uncertainties in $^{40}\text{Ar}/^{39}\text{Ar}$ dating, *Chem. Geol.*, *145*, 117–152, 1998.
- Ruddiman, W. F., M. E. Raymo, D. G. Martinson, B. M. Clement, and J. Backman, Pleistocene evolution: Northern Hemisphere ice sheets and North Atlantic Ocean, *Paleoceanography*, *4*, 353–412, 1989.
- Schrag, D. P., G. Hampt, and D. W. Murray, Pore fluid constraints on the temperature and oxygen isotopic composition of the glacial ocean, *Science*, *272*, 1930–1932, 1996.
- Shackleton, N. J., Oxygen isotopes, ice volume and sea level, *Quat. Sci. Rev.*, *6*, 183–190, 1987.
- Shackleton, N. J., The 100,000-year ice-age cycle identified and found to lag temperature, carbon dioxide, and orbital eccentricity, *Science*, *289*, 1897–1902, 2000.
- Shackleton, N. J., and M. A. Hall, Oxygen and carbon isotope stratigraphy of Deep Sea Drilling Project hole 552A: Plio-Pleistocene glacial history, *Initial Results Deep Sea Drill. Proj.*, *81*, 599–609, 1984.
- Shackleton, N. J., and M. A. Hall, Stable isotope history of the Pleistocene at ODP site 677, *Proc. Ocean Drill. Program Sci. Results*, *111*, 295–316, 1989.
- Shackleton, N. J., A. Berger, and W. A. Peltier, An alternative astronomical calibration of the lower Pleistocene timescale based on ODP Site 677, *Trans. R. Soc. Edinburgh Earth Sci.*, *81*, 251–261, 1990.
- Singer, B. S., and M. S. Pringle, Age and duration of the Matuyama-Brunhes geomagnetic polarity reversal from $^{40}\text{Ar}/^{39}\text{Ar}$ incremental heating analyses of lavas, *Earth Planet. Sci. Lett.*, *139*, 47–61, 1996.
- Tauxe, L., T. Herbert, N. J. Shackleton, and Y. S. Kok, Astronomical calibration of the Matuyama-Brunhes boundary: Consequences for magnetic remanence acquisition in marine carbonates and the Asian loess sequences, *Earth Planet. Sci. Lett.*, *140*, 133–146, 1996.
- Tiedemann, R., M. Samthein, and N. J. Shackleton, Astronomic timescale for the Pliocene Atlantic $\delta^{18}\text{O}$ and dust flux records of Ocean Drilling Program site 659, *Paleoceanography*, *9*, 619–638, 1994.
- Venz, K. A., D. A. Hodell, C. Stanton, and D. A. Warnke, A 1.0 Myr record of glacial North Atlantic intermediate water variability from ODP Site 982 in the northeast Atlantic, *Paleoceanography*, *14*, 42–52, 1999.
- Winograd, I. J., J. M. Landwehr, K. R. Ludwig, T. B. Coplen, and A. C. Riggs, Duration and structure of the past four interglaciations, *Quat. Res.*, *48*, 141–154, 1997.
-
- D. B. Karner, J. Levine, and R. A. Muller, Department of Physics, University of California, Berkeley, CA 94720, USA. (dkarner@socrates.berkeley.edu)
- B. P. Medeiros, Department of Atmospheric Sciences, University of California, Los Angeles, CA 90095, USA.

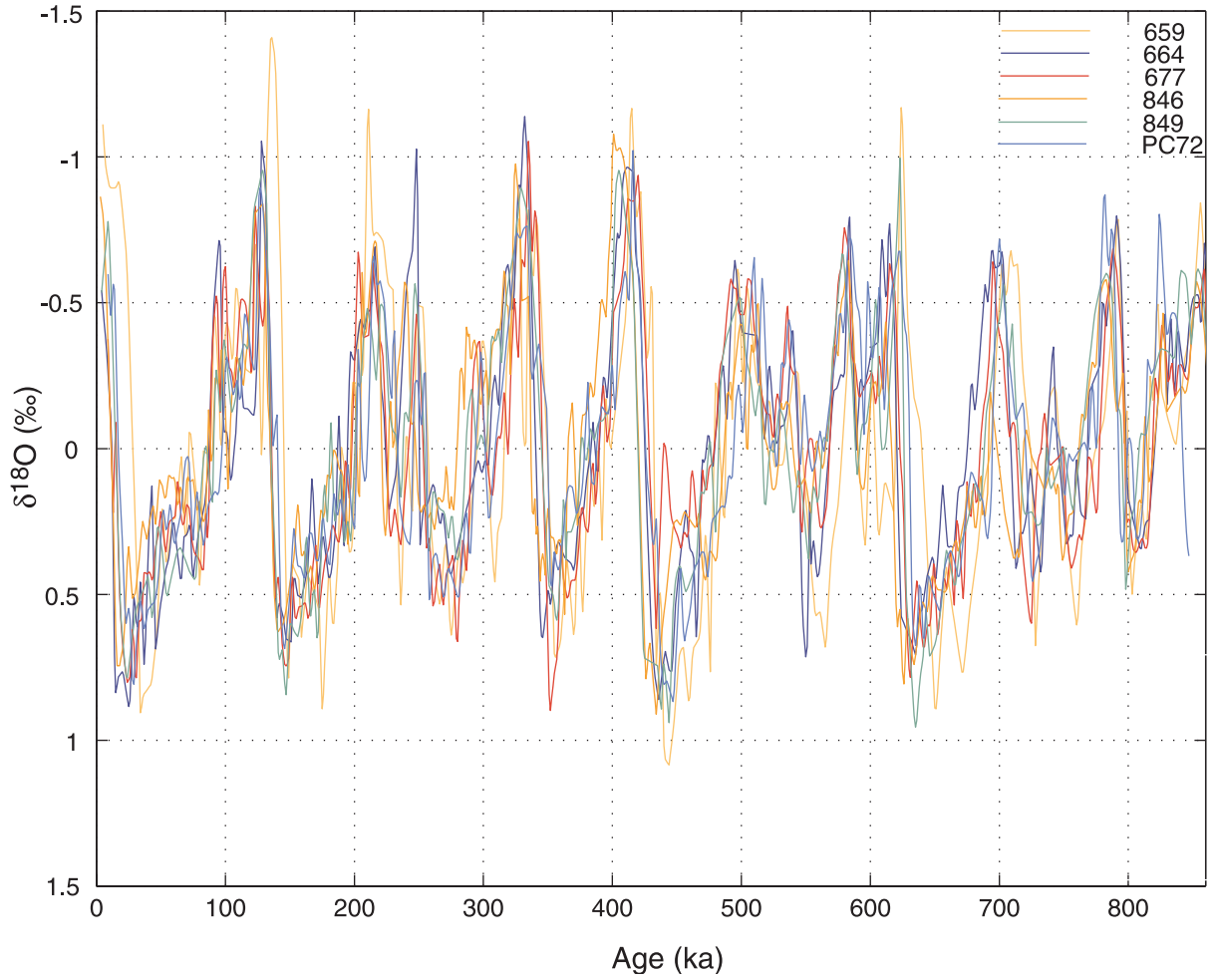


Figure 12. The six obliquity-tuned records from tropical latitudes. These are ODP Sites 659, 664, 677, 846, and 849 and core TT013-PC72. The mean has been subtracted from each, but the amplitudes have not been adjusted. Therefore the spread in the data reflects the true variation in $\delta^{18}\text{O}$ at the seven drilling sites.